JPEDAV (2009) 30:418–428
DOI: 10.1007/s11669-009-9563-5
1547-7037 ©ASM International

Computational Materials Design

Larry Kaufman

(Submitted April 7, 2009)

The program booklet of the 14th National Conference and Multilateral Symposium on Phase Diagrams and Materials Design contained more than 400 pages of papers devoted to the application of computational thermodynamics to the design and use of a wide variety of engineering materials. The work of Professor Jin and his students which displayed many examples of the CALPHAD method featured prominently at this meeting. My presentation illustrated examples in which thermochemical descriptions can be coupled with diffusion data to derive useful practical insight into design of alloys and amorphous and ceramic systems. The wide use of these methods will be enhanced in the future by coordinated investigation of the lattice stability of pure metals and compounds as was illustrated at the conference. Specific directions for such efforts are suggested.

Keywords aqueous corrosion, CALPHAD, computational materials science, lattice stability, martensites, thermochemistry, thermodynamics

1. Introduction

First, I would like to thank the organizers for inviting me to participate in this conference to witness first hand the progress that has been achieved in developing the depth and scope of the phase diagram program in China. The opportunity to visit with my mentor Professor Chang Xu (Chester) Shih was an additional pleasure. When I arrived at MIT in 1952 as a 21-year-old new graduate student, I had the good fortune to work together with Chester in Morris Cohen's Martensite group where exciting measurements were being made on the kinetics of isothermal martensite formation (Fig. 1-3). This topic stimulated my interest in coupling thermodynamics, physical properties and nucleation in order to develop a framework which could be applied to practical problems. I was delighted to see that same philosophy was present in many of the papers at the conference, perhaps it is the influence of Chang Xu Shih in his position as President of the National Natural Science Foundation in guiding the development of these studies in China.

This article is an invited paper selected from participants of the 14th National Conference and Multilateral Symposium on Phase Diagrams and Materials Design in honor of Prof. Zhanpeng Jin's 70th birthday, held November 3-5, 2008, in Changsha, China. The conference was organized by the Phase Diagrams Committee of the Chinese Physical Society with Drs. Huashan Liu and Libin Liu as the key organizers. Publication in *Journal of Phase Equilibria and Diffusion* was organized by J.-C. Zhao, The Ohio State University; Yong Du, Central South University; and Qing Chen, Thermo-Calc Software AB.

Larry Kaufman, CALPHAD, Inc., 140 Clark Road, Brookline, MA 02445-5848. Contact e-mail: larrykaufman@rcn.com.

2. CALPHAD and Computational Thermodynamics

The early years at MIT were enriched by many talented faculty and students, most notably by Mats Hillert who arrived shortly after Chester returned to China and on his return to Sweden became Professor at the Royal Institute of Technology in Stockholm, founded an outstanding group of students from around the world which generated Thermo-Calc and DICTRA software and databases currently used universally. Figures 4-15 illustrate recent applications how the early lessons of Fig. 1-3 have been applied to modern problems. Moreover, it was encouraging to see how CALPHAD methods have been applied to problems of interest in China.[1] On the other hand, I became aware of the outstanding work of Zhangpeng Jin and Yong Du[9,10] long before I met them in person. However, the present conference booklet[11-22] displays more than a dozen important studies that Jin and more than 30 student colleagues have performed. These cover a wide range of scientific and engineering topics including amorphous Al-Fe-Zr alloys,[11] first-principles assisted assessments of Au-Co-Sn[12] and Al-Fe-Zr,[13] thermodynamics and CALPHAD modeling of TiO_2-Y_2O_3,[14] B-C-Si,[15] Gd-Zn,[16] and Mg-Hg-Ga,[17] age-hardening of Ti-Al-N coatings,[18] experimental determination of Ni-Si-Zn ternary system,[19] CALPHAD study of Mg-Ag-Ca,[20] CALPHAD study of Fe-Nd-B and applications to sintering, metal spinning and levitation melting,[21] and predictions of interfacial reaction in multicomponent systems.[22]

The description of the Pu-Ga system[5] shown in Fig. 5 and 6[5] flow directly from Fig. 1-3 and the CALPHAD schematic of Fig. 4. The lesson of Fig. 1 and 2 that was applied in Fig. 6 is that the small values of the activation energies that are mandated when pure isothermal martensitic (diffusionless) transformations are observed at very low temperatures require pre-existing embryos or nucleation sites. Thus, the same models were employed in calculating Fig. 5 and 6 as those used in Fig. 1-3. The only difference is

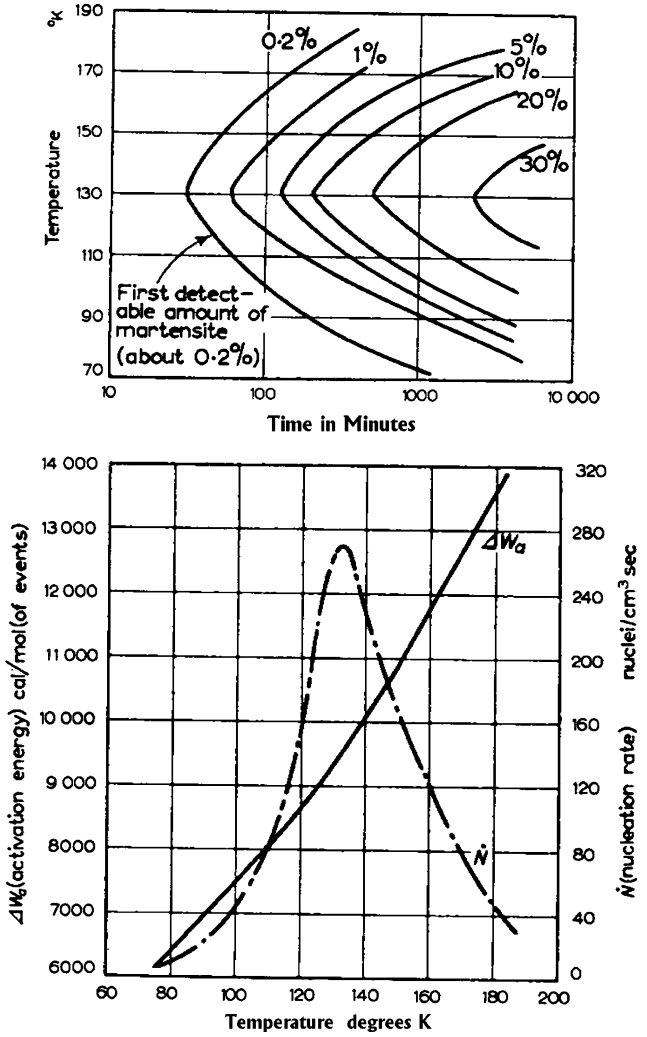

Fig. 1 Measured activation energy and kinetics of isothermal martensite formation in an Fe-Ni-Mn alloy[2]

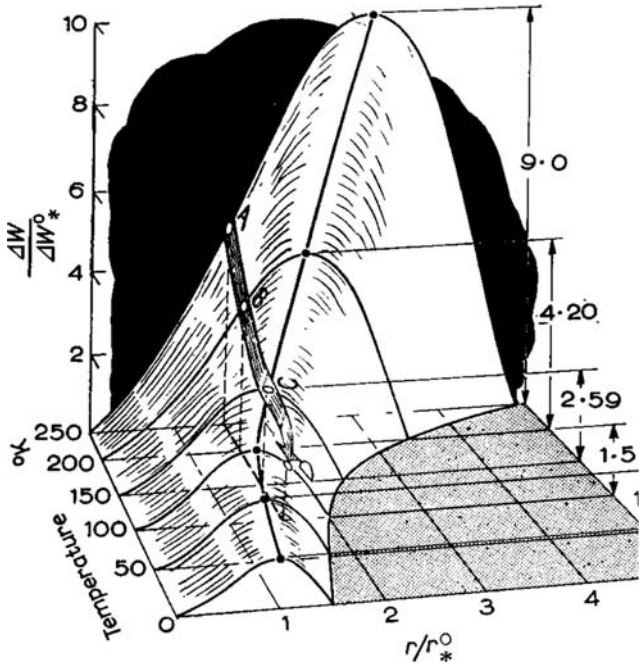

Fig. 2 The activation energy of formation calculated for a martensite embryo in an Fe-30Ni alloy[3]

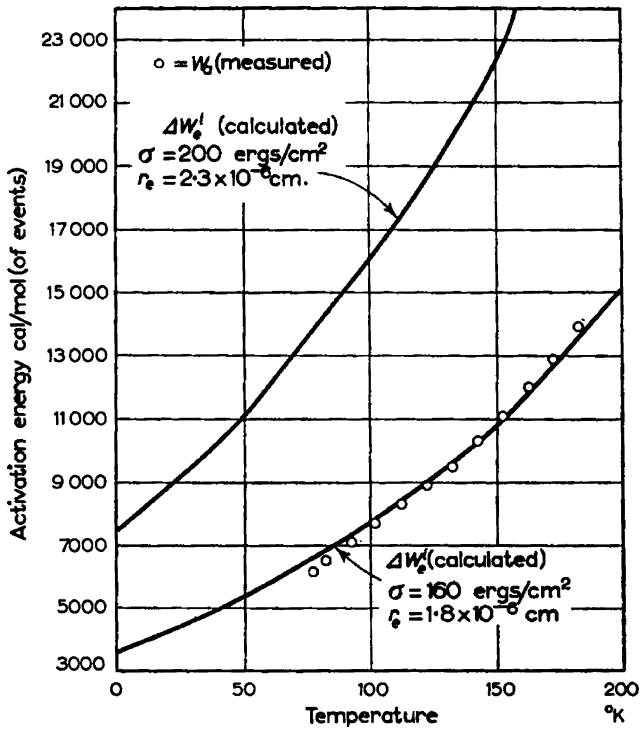

Fig. 3 Calculated and measured activation energy for isothermal martensite formation in an Fe-Ni-Mn alloy as a function of embryo radius size and interfacial energy between the parent fcc phase and daughter bcc phase[3]

that there are two different daughter phases in the Pu-Ga[5] case. The case for pre-existing embryos or heterogeneous nucleation has been strengthened recently by the observations of "particle size effects" wherein the M_S temperature has been lowered or eliminated by examining small and smaller size austenite particles or cooling at higher and higher cooling rates.

Application of the CALPHAD method for calculation of the sigma, P-Phase and Ni_2Cr phase in the Ni-Cr-Mo based C-22 alloys[4,6] using Thermo-Calc and DICTRA software and databases is illustrated in Fig. 7.[6] The essential feature of this analysis was to characterize the stability of the fcc phase with respect to Ni_2Cr at low temperature for long times displayed in Fig. 7.

Figures 8-13 apply the same techniques for investigation of the fabrication and application of amorphous iron coatings for large waste package structures in repository settings.[7] This problem posed several additional challenges since the amorphous alloys contained Fe-Cr-Mo-B and C and although ThermoCalc databases are available for the liquid phase and for the M_3B phases, which were chosen to be surrogates for the amorphous and devitrification

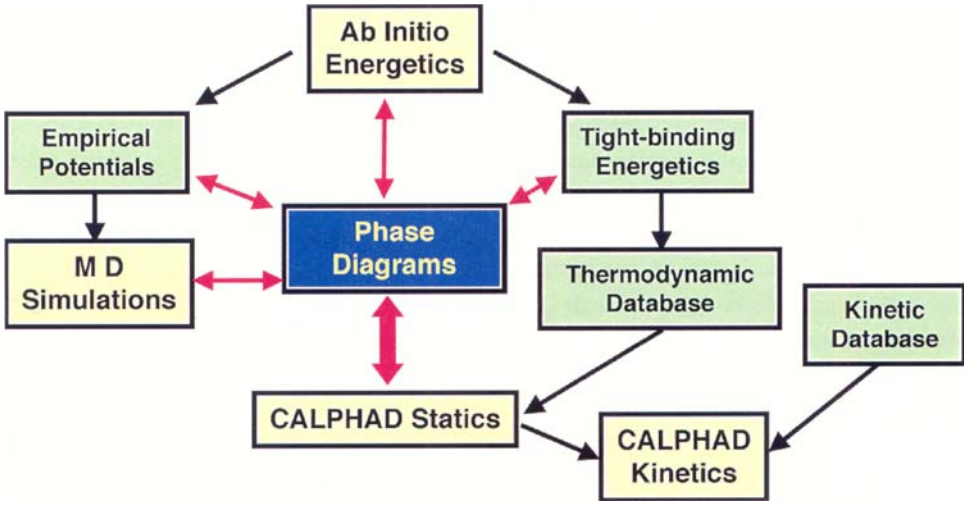

Fig. 4 Schematic representation of a flowchart for integrated description of phase stability and transformations[4]

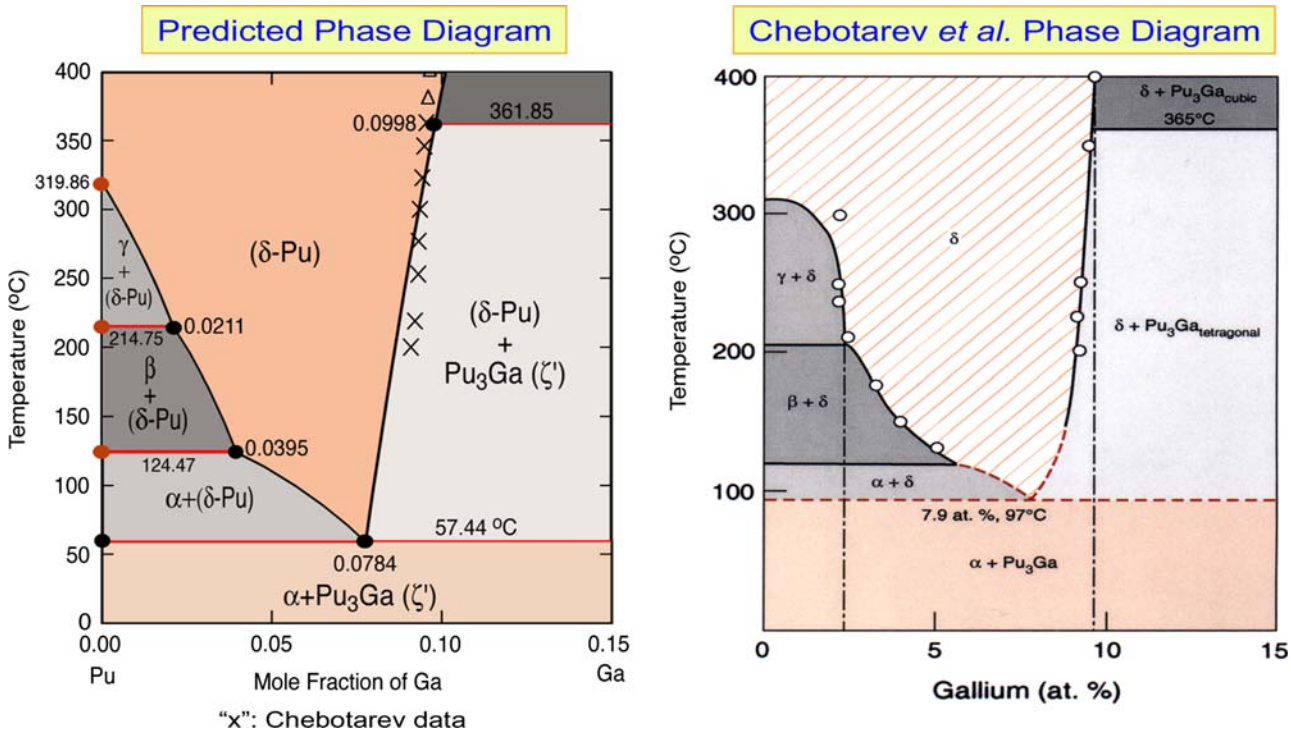

Fig. 5 Calculated and experimental measurements of the Pu-Ga eutectoid[5]

nucleation phase, the corresponding DICTRA mobility database is more limited. CALPHAD modeling was used in combination with experimental studies to estimate the missing diffusion coefficients and the results in Fig. 8 and 9 for alloy SAM7. The upper panels in Fig. 8 show the relation between time-temperature and cooling rate on the left and fraction of the devitrification phase, time and cooling rate on the right. The second panel down on the left shows the same results except that the abscissa is temperature instead of time. These three panels display the effects of cooling rate on devitrification. The fraction of devitrification phase decreases toward zero as the cooling rate increases. However, the T_{limit}, which is the lower limit for devitrification, independent of cooling rate. The lower five panels of Fig. 8 and upper 4 panels of Fig. 9 show the fraction transformed as a function of time at various temperatures. The final (large panel) of Fig. 9 collects the kinetic of devitrification (formation of M_3B) as a function of

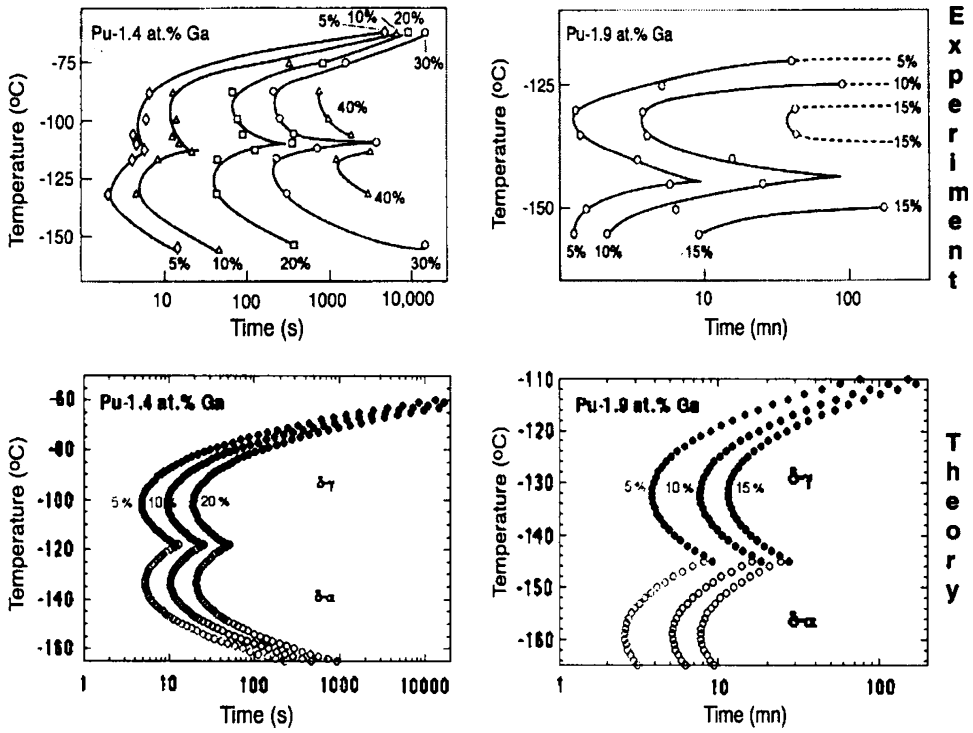

Fig. 6 Martensitic transformation in Pu-Ga alloys calculated with the same models used in Fig. 1-3

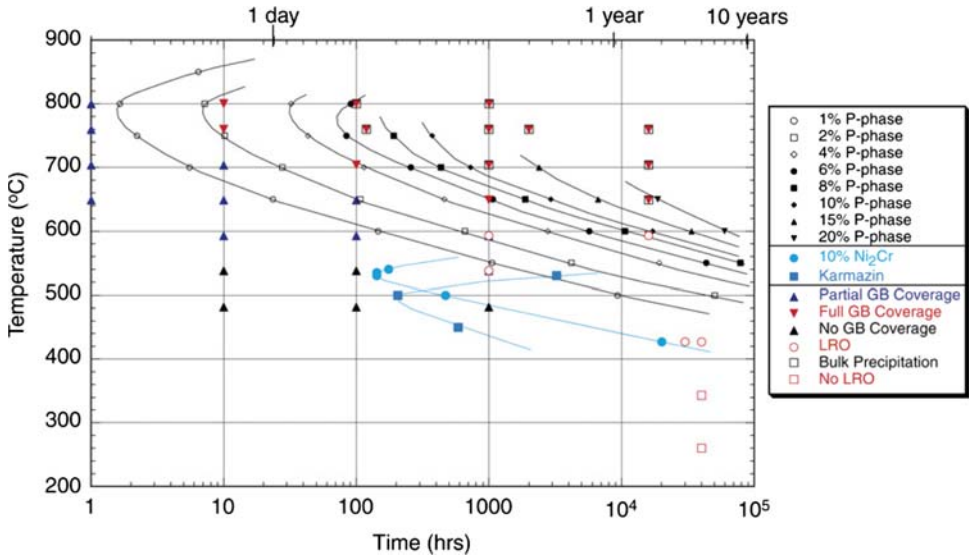

Fig. 7 Calculated and experimental kinetics of formation of P phase and Ni_2Cr phase in alloy C-22[6]

time. Comparison of Fig. 9 and 7 provides some physical insight into the kinetics of two different processes: Figure 7 for the formation of sigma, P-Phase and Ni_2Cr from a fcc parent phase on cooling and Fig. 9 for the formation of a devitrification phase (M_3B) from an amorphous (liquid) phase. In both cases, there is a limiting temperature T_{limit} above which the daughter phase is not stable. Thus, T_{limit} is defined by the thermodynamic properties of the system. The time-temperature-transformation "C-Curves" in Fig. 7 and 9 depend on the thermodynamics and the mobility of the components and the effectiveness of the nucleation phase. The critical cooling rate required to retain SAM7 liquid is about 60 °C/s which corresponds to a level of 1.1% of the devitrification phase. Finally, it is interesting to compare the

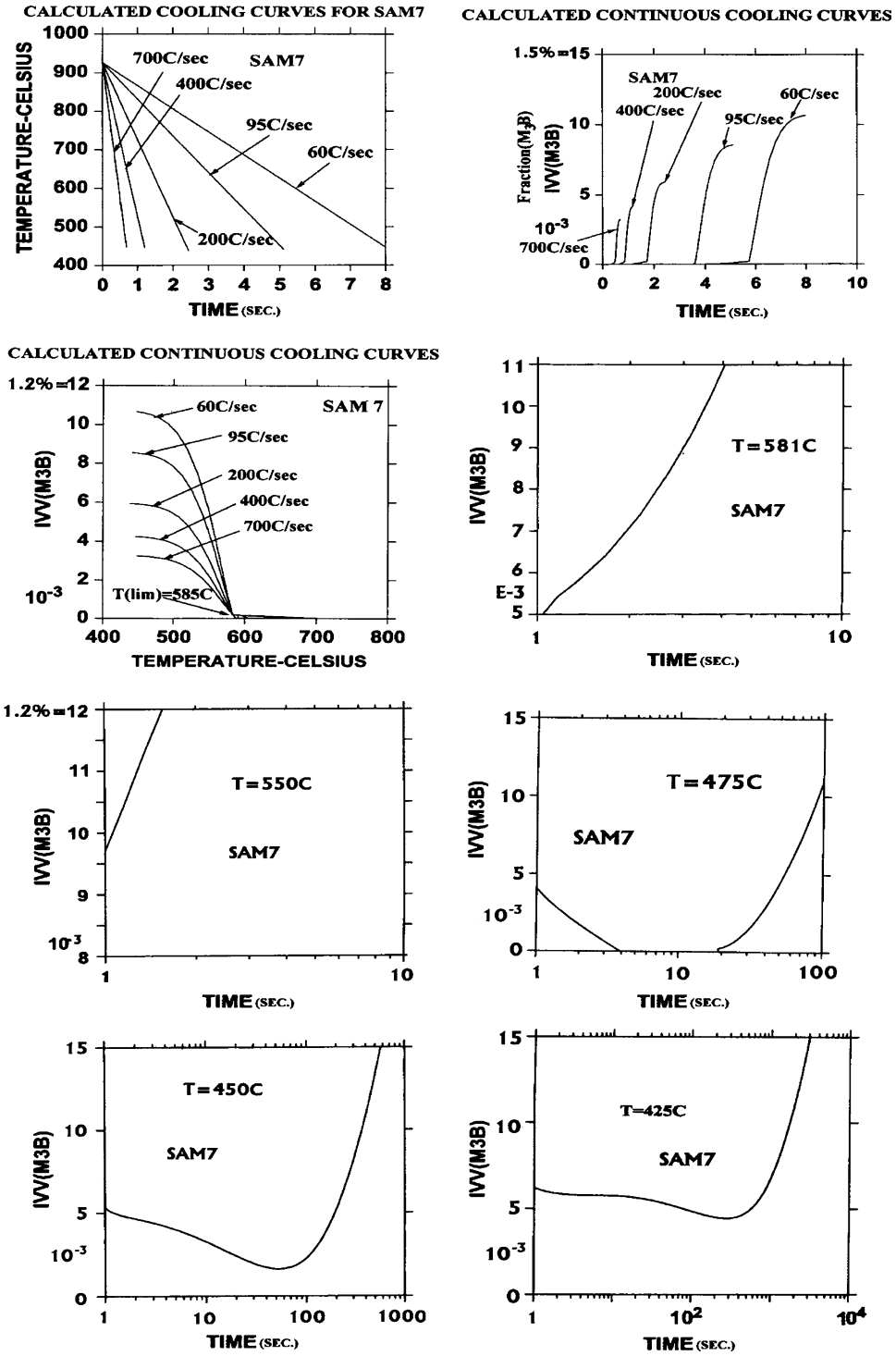

Fig. 8 Calculated kinetics of devitrification for amorphous Fe-B-C-Mo-W alloy SAM7[7]

current results for the mobility of B, C, Fe, Cr and Mo used in the current calculations[7] with the correlations developed by Faupel et al.[23] shown in Fig. 10, which indicates that the descriptions that are required to describe the observed formation and devitrification of amorphous iron alloys are in general accordance with comparable observations on other alloy systems.

The corrosion resistance of amorphous iron coatings offer substantial performance and cost savings as compared with other high-performance corrosion-resistant materials.

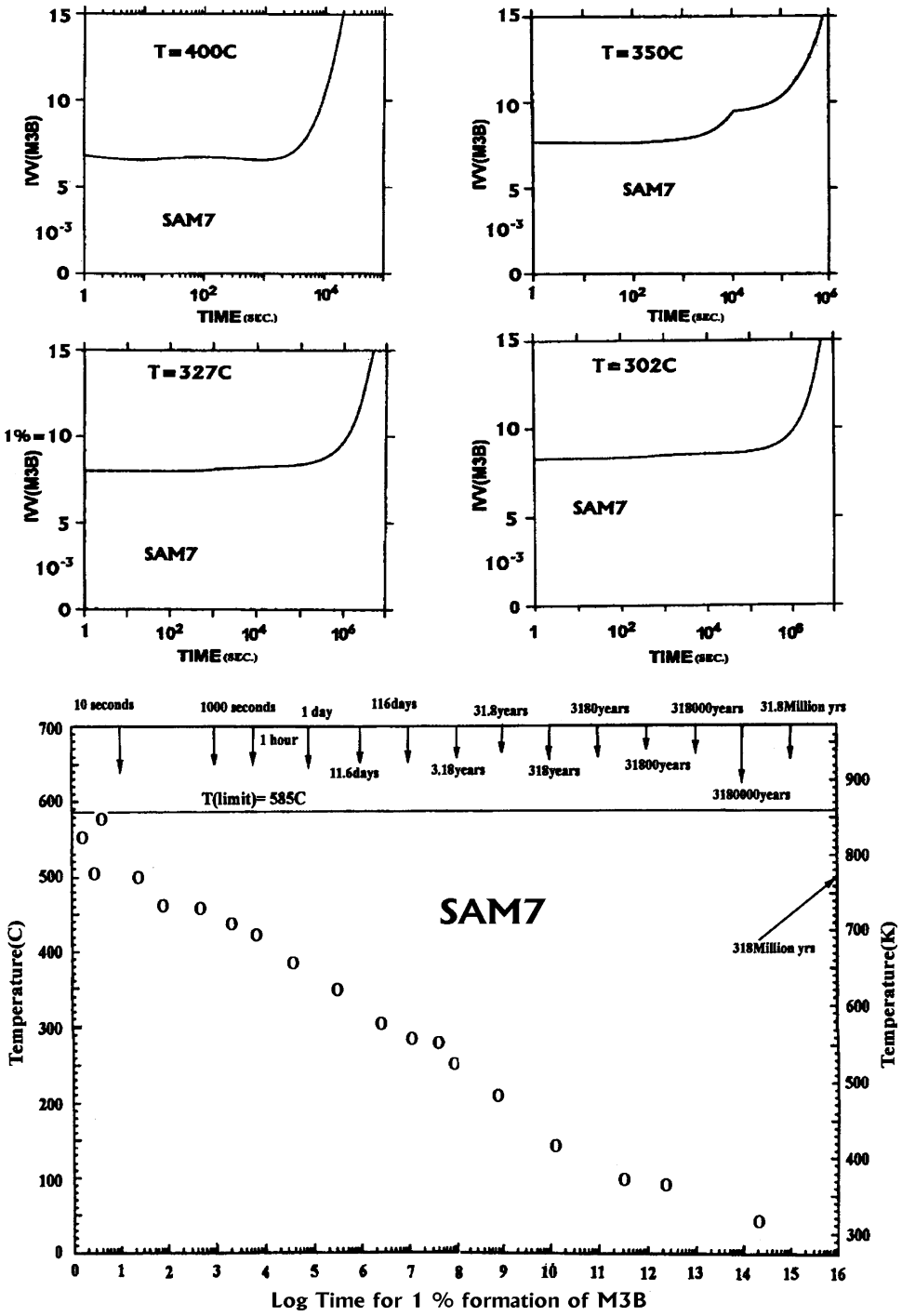

Fig. 9 Calculated kinetics of devitrification for amorphous Fe-B-C-Mo-W alloy SAM7[7]

Figures 11-13 show experimental measurements and calculations of the corrosion behavior of SAM40 which is an amorphous Fe-Cr-Mo-B-C alloy.[7] Figure 11 shows the results of cyclic polarization measurements at 90 °C in seawater at pH = 6.4 for an amorphous melt spun ribbon that was annealed at 600 °C for 5 min before cyclic polarization testing. Based on the results of Fig. 9 this sample would have undergone some devitrification. The experimental measurements are presented in terms of the Ag/AgCl standards while the calculations performed with Thermo-Calc software are presented in terms of the V_{she}. Figure 12 makes the translation showing both on the same Fig. 12. Figure 13 shows the calculated Pourbaix diagram for SAM40 in seawater at 90 °C.

Figures 14 and 15 show how the CALPHAD method can be applied to help archeological studies. The calculations were performed in support of field work performed by Professor Heather Lechtman at MIT. Professor Lechtman has studied early South American cultures near the Andean city of Tiwanaku near the southern shores of Lake Titicaca. The center of the city was a temple constructed as a pyramid mound. At the summit was a central unroofed, sunken court that collected large volumes of water during the annual, 4-month season of torrential rains. Stone-lined canals drained the water from the sunken court through an elaborate drainage system of channels that served the city. Portions of the canals are preserved in the pyramid. The vertical walls are constructed of carefully cut sandstone blocks that abut without mortar. Figure 14 shows an exit portion of one of the canals. The composition of the cramp was measured as Cu-6wt.%As-5.8wt.%Ni containing a ternary AsCuNi phase which comprised 21% by volume. The CALPHAD analysis was employed to estimate the melting temperature as about 900 °C so that the shrinkage on solidification in the forms cut from the blocks would provide a strong clamping force to prevent water leaking between the joints. A similar analysis of shards from a 3000-year-old Persian copper smelting crucible was recently completed containing SiO_2-Al_2O_3-Fe_3O_4-CaO-MgO and calculated to melt at 1160 °C in agreement with measurements.

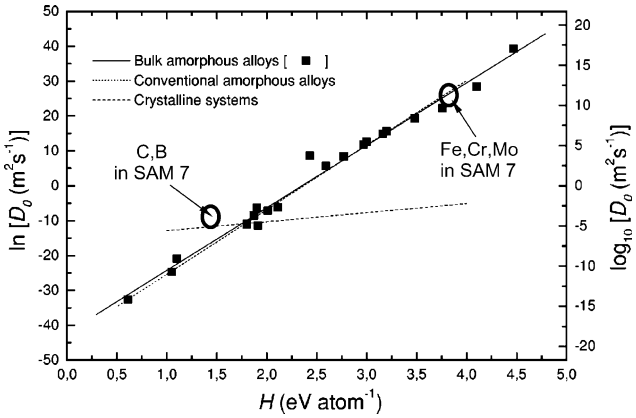

Fig. 10 Comparison of calculated mobilities for Fe, Cr, Mo, B and C used in the calculation of devitrification kinetics of SAM7[7] with correlation proposed by Faupel et al.[23]

3. Concluding Remarks

The examples presented in this article show that the CALPHAD method has been extremely successful in finding a wide range of applications. The concept of lattice stability has played an essential role in the establishment of the general CALPHAD methodology and in establishing a framework that is now accepted worldwide. Comparisons of the lattice stabilities, or structural energy differences, for the bcc, hcp, and fcc phases for the elements derived by ab initio and CALPHAD interpolation methods generally yield good agreement. However, substantial differences exist for elements in the Nb, Mo, Ru, and Rh columns of the periodic table. Sundman et al.[24] have suggested that it

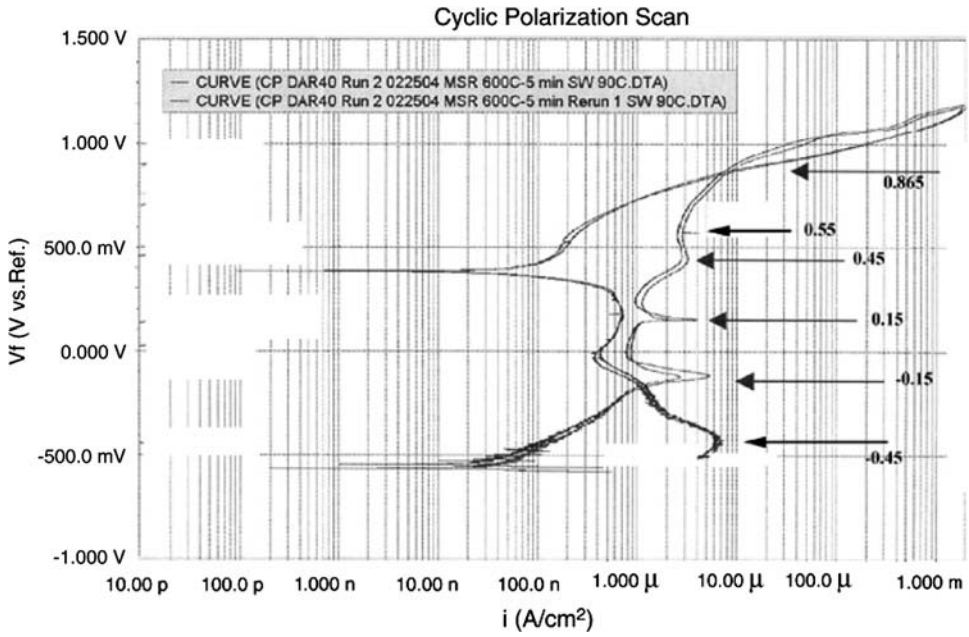

Fig. 11 Cyclic polarization measurements of an amorphous melt spun ribbon of alloy SAM40 in seawater at pH = 6.4 and 90 °C after annealing for 5 min at 600 °C. The ordinate is voltage relative to an Ag/AgCl standard corresponding to those noted in Fig. 12 (Hematite is Fe_2O_3)[7]

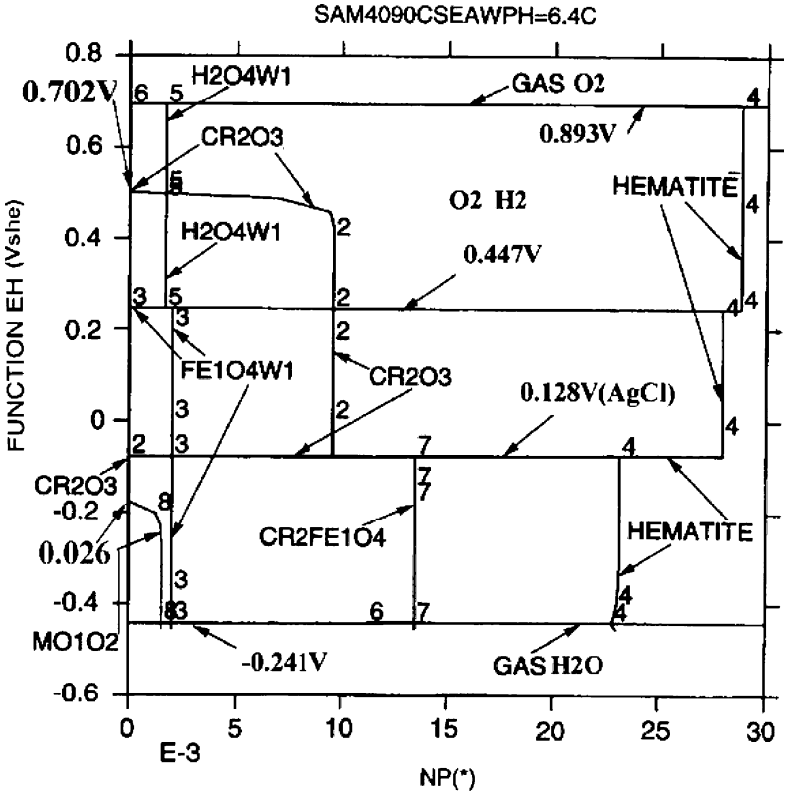

Fig. 12 Calculated voltage, EH vs. phase fraction (NP) in SAM40 alloy in seawater at 90 °C at pH = 6.4. Voltages are noted relative to a Ag/AgCl standard as displayed in Fig. 11 (Hematite is Fe_2O_3)[7]

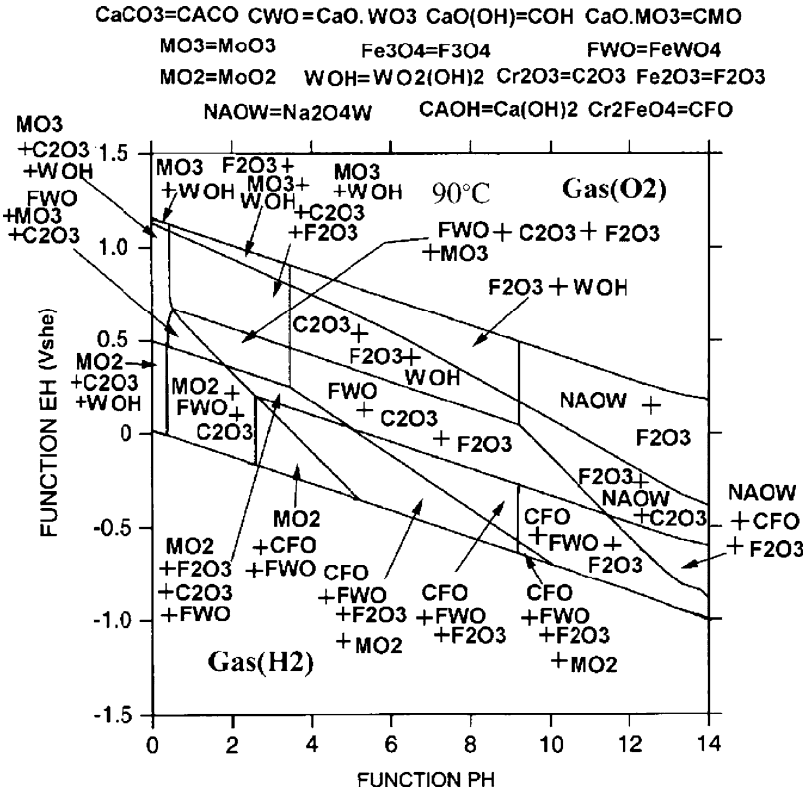

Fig. 13 Calculated Pourbaix diagram for SAM40 alloy in seawater at 90 °C (Hematite is Fe_2O_3)[7]

would be appropriate to revisit the topic of lattice stabilities in a more general and systematic way dealing with many more structures than was contemplated originally.[25] I heartily endorse this suggestion. Moreover, it is very important that all methods that are currently available be employed to derive the best possible "3rd generation" lattice stability values as emphasized in Ref 24. The extensive comparison of CASTEP-GGA and VASP-GGA presented by Tao et al.[26] presents a rather narrow view of the lattice stability of Fe, Ru and Os in contrast to the inclusive considerations presented by the CALPHAD method.[24,25,27-31] Consequently, it is not surprising to find that the results of the CASTEP-GGA, as compared in Table 1 to the empirical results, suggest that hcp Fe is *more* stable than bcc Fe by 37942 J/mol and more stable than fcc Fe by 7992 J/mol. These values are 10-20 times larger than the values that have been demonstrated by experiment and the hcp-bcc value has a wrong sign. No explanation is given for these findings. Similar inconsistencies can be seen for Ru and Os and for the VASP-GGA values[26] except that the latter has a bcc Fe more stable than hcp Fe at zero K and one atmosphere. These results show that one needs to be very careful in dealing with the lattice stabilities and a

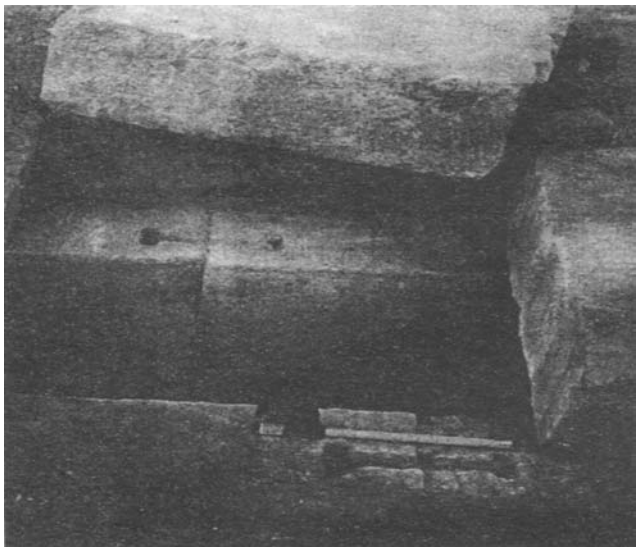

Fig. 14 Photograph of a canal capping stone and an I-socket As-Cu-Ni metal cramp from the early period of the Middle Horizon in the southern Andes (ca. AD 400-800) at the site of Tiwanaku, Bolivia. The capping stone has been slid out of place to reveal two in situ I-sockets and metal cramps located in the side walls. The sockets are chiseled into the upper faces of abutting vertical blocks, as either side of their common joint. The length of one socket, as indicated by the scale, is approximately 19.5 cm

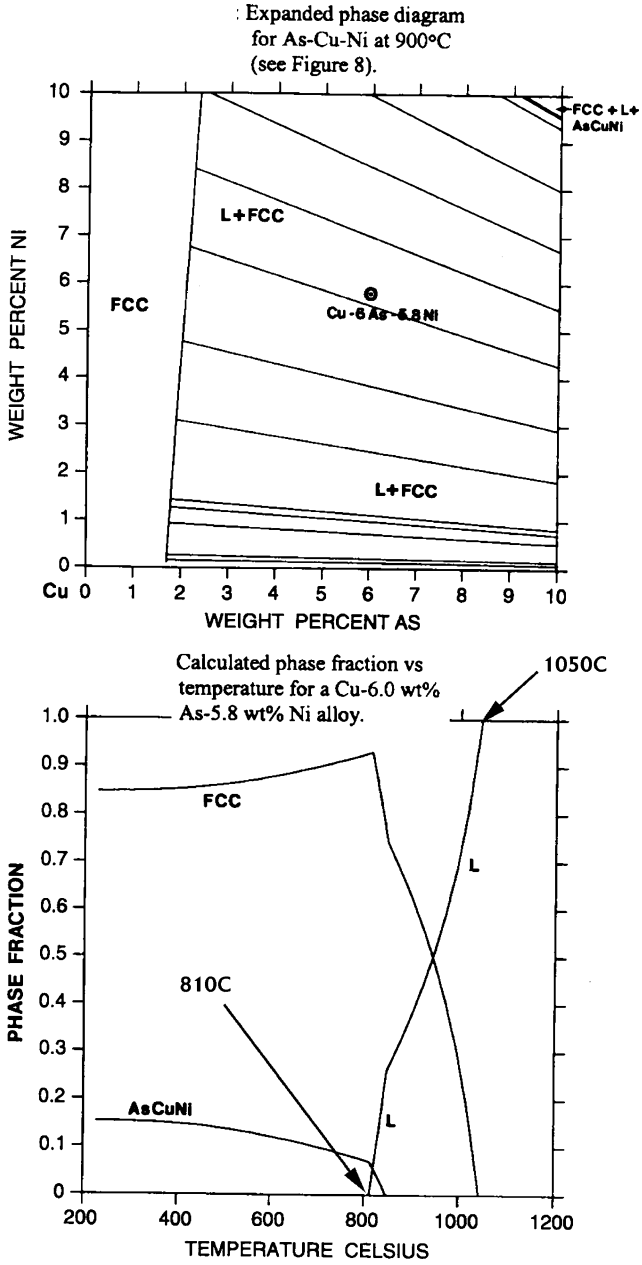

Fig. 15 Calculated and experimental phase equilibria in the As-Cu-Ni system[8]

Table 1 Comparison of lattice stabilities after Tao et al. by CASTEP-GGA with CALPHAD and empirical values (all data in J/mol and are relative to the hcp structure)

	CASTEP-GGA	CALPHAD-EMPIRICAL	CASTEP-GGA	CALPHAD-EMPIRICAL
Fe	bcc 37942	bcc −5452[27-29]	fcc 7992	fcc 640 [27-29]
Ru	bcc 61107	bcc 6400[28-30]	fcc 11086	fcc 500 [28-30]
Os	bcc 85468	bcc 4736 [28,29]	fcc 13349	fcc 552 [28,29]

coordinated effort to the "3rd generation" lattice stability values are highly desirable.

References

1. *Program Booklet of the 14th National Conference and Multilateral Symposium on Phase Diagrams and Materials Design*, Changsha, China, November 3-5, 2008, which was sponsored by the Phase Diagram Committee of the Chinese Physical Society and the Central South University
2. C. Shih, B.L. Averbach, and M. Cohen, Isothermal Martensitic Transformation in an Fe-Ni-Mn Alloy, *Trans. AIME*, 1995, **205**, p 183-190
3. L. Kaufman and M. Cohen, Thermodynamics and Kinetics of Martensitic Transformations, *Prog. Met. Phys.*, 1958, **7**, p 165-246
4. P.E.A. Turchi, L. Kaufman, and Z.-K. Liu, Modeling of Ni-Cr-Mo Base Alloys, Part I—Phase Stability, *CALPHAD*, 2006, **30**, p 70-87
5. P.E.A. Turchi, L. Kaufman, S. Zhou, and Z.-K. Liu, Thermostatics and Kinetics of Transformations in Pu-Based Alloys, *J. Alloys Compd.*, 2007, **444**, p 28-35
6. P.E.A. Turchi, L. Kaufman, and Z.-K. Liu, Modeling of Ni-Cr-Mo Base Alloys, Part II—Kinetics, *CALPHAD*, 2007, **31**, p 237-248
7. L. Kaufman, J.H. Perepezko, K. Hildal, J. Farmer, D. Day, N. Yang, and D. Branagan, Transformation, Stability and Pourbaix Diagrams for High Performance Corrosion Resistant (HPCRM) Alloys, *CALPHAD*, 2009, **33**, p 89-99
8. S. Uhland, H. Lechtman, and L. Kaufman, Assessment of the As-Cu-Ni System: An Example From Archeology, *CALPHAD*, 2001, **25**, p 109-124
9. Y. Du, Z.P. Jin, and P. Huang, Thermodynamic Assessment of the ZrO_2-$YO_{1.5}$ System, *J. Am. Ceram. Soc.*, 1991, **74**, p 1569-1577
10. Y. Du, Z.P. Jin, and P. Huang, Thermodynamic Calculation of the ZrO_2-$YO_{1.5}$-MgO System, *J. Am. Ceram. Soc.*, 1991, **74**, p 2107-2112
11. H. Chen, Y. Liu, C. Fan, Y. Ouyang, X. Zhong, Y. Du, and Z.P. Jin, The Composition Range of Amorphous Forming for Al-Fe-Zr, *The Program Booklet of the 14th National Conference and Multilateral Symposium on Phase Diagrams and Materials Design*, Changsha, China, November 3-5, 2008, p 13-18
12. H.Q. Dong, X.M. Tao, L.G. Zhang, J.S. Wang, H.S. Liu, and Z.P. Jin, First-Principles Calculation Assisted Thermodynamic Assessment of the Au-Co-Sn Ternary System, *The Program Booklet of the 14th National Conference and Multilateral Symposium on Phase Diagrams and Materials Design*, Changsha, China, November 3-5, 2008, p 31
13. Y. Ouyang, F. Guo, F. Liu, Y. Du, and Z.P. Jin, The Thermodynamic Properties of the Al-Fe-Zr System Calculated with First Principles, *The Program Booklet of the 14th National Conference and Multilateral Symposium on Phase Diagrams and Materials Design*, Changsha, China, November 3-5, 2008, p 110
14. W. Gong, D. Li, Y. Liu, B. Wang, and Z.P. Jin, Thermodynamic Investigation of the TiO_2-ZrO_2 System, *The Program Booklet of the 14th National Conference and Multilateral Symposium on Phase Diagrams and Materials Design*, Changsha, China, November 3-5, 2008, p 40
15. H.M. Chen, F. Zheng, L.B. Liu, and Z.P. Jin, Thermodynamic Optimization of the B-C-Si System, *The Program Booklet of the 14th National Conference and Multilateral Symposium on Phase Diagrams and Materials Design*, Changsha, China, November 3-5, 2008, p 43
16. H.Y. Qi, L.B. Liu, L.B. Zhang, G.X. Zhang, and Z.P. Jin, Thermodynamic Assessment of the Gd-Zn Binary System, *The Program Booklet of the 14th National Conference and Multilateral Symposium on Phase Diagrams and Materials Design*, Changsha, China, November 3-5, 2008, p 118
17. Y. Feng, R. Wang, H. Liu, J.S. Wang, and Z.P. Jin, Measurement and Thermodynamic Assessment of Phase Relations the Mg-Hg-Ga Ternary System, *The Program Booklet of the 14th National Conference and Multilateral Symposium on Phase Diagrams and Materials Design*, Changsha, China, November 3-5, 2008, p 265
18. L. Chen, Y. Du, P.H. Mayrhofer, S.P. Wang, P. Li, J. Li, and Z.P. Jin, The Influence of Age-Hardening on Turning and Milling Performance of Ti-Al-N Coated Inserts, *The Program Booklet of the 14th National Conference and Multilateral Symposium on Phase Diagrams and Materials Design*, Changsha, China, November 3-5, 2008, p 66
19. H. Xu, Y. Du, L. Zhang, G.P. Wang, and Z.P. Jin, Phase Equilibria of the Ni-Si-Zn Ternary System at 600°C, *The Program Booklet of the 14th National Conference and Multilateral Symposium on Phase Diagrams and Materials Design*, Changsha, China, November 3-5, 2008, p 191
20. G.H. Wang, L.G. Zhang, H.Y. Qi, L.B. Liu, and Z.P. Jin, Experiment Coupled with Modeling to Establish the Mg-Rich Phase Equilibria of Mg-Ag-Ca, *The Program Booklet of the 14th National Conference and Multilateral Symposium on Phase Diagrams and Materials Design*, Changsha, China, November 3-5, 2008, p 278
21. Y. Feng, R. Wang, H. Liu, J.S. Wang, and Z.P. Jin, Thermodynamic Description of Fe-Nd-B Ternary System and Its Applications, *The Program Booklet of the 14th National Conference and Multilateral Symposium on Phase Diagrams and Materials Design*, Changsha, China, November 3-5, 2008, p 289
22. H.S. Liu, W.J. Zhu, X.M. Tao, and Z.P. Jin, Prediction of Interfacial Reactions in Multicomponent System, *The Program Booklet of the 14th National Conference and Multilateral Symposium on Phase Diagrams and Materials Design*, Changsha, China, November 3-5, 2008, p 310
23. F. Faupel, W. Frank, M.-P. Macht, H. Mehrer, V. Naundorf, K. Ratzke, H.R. Schober, S.K. Sharma, and H. Teichler, Diffusion in Metallic Glasses and Supercooled Melts, *Rev. Modern Phys.*, 2003, **75**, p 237-280
24. B. Sundman, N. Dupin, and Q. Chen, The 3rd Generation Thermodynamic Database, *The Program Booklet of the 14th National Conference and Multilateral Symposium on Phase Diagrams and Materials Design*, Changsha, China, November 3-5, 2008, p 132
25. L. Kaufman, The Lattice Stability of the Transition Metals, *Phase Stability in Metals and Alloys*, P.S. Rudman, J.S. Stringer, and R.I. Jaffe, Ed., McGraw-Hill Book Co., New York, NY, 1967, p 125-149
26. H.J. Tao, J. Yin, and B.Y. Huang, First Principles Study on the Lattice Stability of Elemental Fe, Ru and Os in the VIIIB Group, *The Program Booklet of the 14th National Conference and Multilateral Symposium on Phase Diagrams and Materials Design*, Changsha, China, November 3-5, 2008, p 143-155
27. Q. Chen and B. Sundman, Modeling of Thermodynamic Properties for BCC, FCC, Liquid and Amorphous Iron, *J. Phase Equilib.*, 2001, **22**, p 631-644

28. L. Kaufman and H. Bernstein, *Computer Calculation of Phase Diagrams*, Academic Press, New York, NY, 1970
29. L. Kaufman, The Lattice Stability of the Iron Group Elements, *Scand. J. Met.*, 1991, **20**, p 32-38
30. A.E. Kissavos, S. Shallcross, V. Meded, L. Kaufman, and I. Abrikosov, A Critical Test of Ab Initio and CALPHAD Methods: The Structural Energy Difference Between BCC and HCP Mo, *CALPHAD*, 2005, **29**, p 17-23
31. C. Akser, A.B. Belonoshko, A.S. Mikhaylushkin, and I. Abrikosov, First-Principles Solution to the Problem of the Mo Lattice Stability, *Phys. Rev.*, 2008, **B77**, p 220102(R)